Geophysical Research Letters

RESEARCH LETTER
10.1029/2018GL080301

Key Points:
- Three eruptive phases are characterized in detail through five years of high-frequency monitoring
- We identify and discuss precursors to phreatic and phreatomagmatic eruptions
- Enhanced hydrothermal sealing can lead to larger eruptions and top-down remobilization of magma

Supporting Information:
- Supporting Information S1

Correspondence to:
J. M. de Moor,
maartenjdemoor@gmail.com

Citation:
de Moor, J. M., Stix, J., Avard, G., Muller, C., Corrales, E., Diaz, J. A., et al. (2019). Insights on hydrothermal-magmatic interactions and eruptive processes at Poás volcano (Costa Rica) from high-frequency gas monitoring and drone measurements. *Geophysical Research Letters*, *46*, 1293–1302. https://doi.org/10.1029/2018GL080301

Received 31 AUG 2018
Accepted 14 JAN 2019
Accepted article online 18 JAN 2019
Published online 6 FEB 2019

The copyright line for this article was changed on 29 JUL 2019 after original online publication.

Insights on Hydrothermal-Magmatic Interactions and Eruptive Processes at Poás Volcano (Costa Rica) From High-Frequency Gas Monitoring and Drone Measurements

J. M. de Moor[1,2], J. Stix[3], G. Avard[1], C. Muller[1], E. Corrales[4], J. A. Diaz[4], A. Alan[4], J. Brenes[1], J. Pacheco[1], A. Aiuppa[5], and T. P. Fischer[2]

[1]Observatorio Vulcanológico y Sismológico de Costa Rica, Universidad Nacional, Heredia, Costa Rica, [2]Department of Earth and Planetary Sciences, University of New Mexico, Albuquerque, NM, USA, [3]Department of Earth and Planetary Sciences, McGill University, Montreal, Québec, Canada, [4]Gas Sensing Lab, CICANUM, Physics School, Universidad de Costa Rica, San José, Costa Rica, [5]Dipartimento DiSTeM, Università di Palermo, Palermo, Italy

Abstract Identification of unambiguous signals of volcanic unrest is crucial in hazard assessment. Processes leading to phreatic and phreatomagmatic eruptions remain poorly understood, inhibiting effective eruption forecasting. Our 5-year gas record from Poás volcano, combined with geophysical data, reveals systematic behavior associated with hydrothermal-magmatic eruptions. Three eruptive episodes are covered, each with distinct geochemical and geophysical characteristics. Periods with larger eruptions tend to be associated with stronger excursions in monitoring data, particularly in SO_2/CO_2 and SO_2 flux. The explosive 2017 phreatomagmatic eruption was the largest eruption at Poás since 1953 and was preceded by dramatic changes in gas and geophysical parameters. The use of drones played a crucial role in gas monitoring during this eruptive period. Hydrothermal sealing and volatile accumulation, followed by top-down reactivation of a shallow previously emplaced magma body upon seal failure, are proposed as important processes leading to and contributing to the explosivity of the 2017 eruption.

Plain Language Summary High-frequency monitoring of phreatic eruptions shows that clear precursory signals often exist to these dangerous explosive events. We interrogate the processes that lead to phreatic eruptions and investigate the intricate connections between magma intrusions and the hydrothermal systems that they feed.

1. Introduction

Phreatic eruptions are common occurrences at wet volcanoes. Key questions regarding volcanic hazard assessment of these events are the role of magma and whether or not they are precursors to larger-magmatic eruptions (e.g., Barberi et al., 1992; Rouwet et al., 2014; Stix & de Moor, 2018). Part of the problem in understanding and predicting eruptions involving magmatic and hydrothermal interactions is the diversity of potential processes in operation, including magma intrusion (e.g., Mt. St. Helens 1980 eruption; Cashman & Hoblitt, 2004, and Ontake volcano 2007 eruption; Nakamichi et al., 2009), injection of magmatic gas into the hydrothermal system (e.g., White Island 2012 eruption; Christenson et al., 2017; Poás 2014; de Moor, Aiuppa, Pacheco, et al., 2016), hydrothermal sealing (e.g., Ruapehu, 2007; Christenson et al., 2010), infiltration of meteoric water (e.g., Mt St Helens 1989–1991; Mastin, 1994), and hydrothermal system response to Earth tides (Girona et al., 2018). Detailed multidisciplinary study of these systems is needed to better understand the processes leading to eruption in order to inform hazard assessment.

Poás volcano (10.1977°N 84.2310°W) is one of the most active volcanoes in Central America and is one of the best places in the world to study phreatic eruptions and dynamic interactions between magmatic gases and hydrothermal fluids. The crater typically hosts a warm hyper-acid lake (pH < 1, ~50 °C; Martínez et al., 2000; Rowe et al., 1992), which frequently produces small phreatic eruptions. In April 2017 the volcano produced larger VEI 2 phreatic to phreatomagmatic eruptions, the most significant activity since 1955 (Figure S1 in the supporting information; Salvage et al., 2018). Poás was visited by ~500,000 tourists per year (before the 2017 eruption) and is located just 22 km north of the heavily populated Central Valley (~3.5 million people) and SJO international airport. The acid lake is the shallow manifestation of an extensive hydrothermal system

fed by magmatic gases (Rowe et al., 1992). Pools of liquid S were observed on the floor of the desiccated lake in the late 1980s (Oppenheimer & Stevenson, 1989), a phenomenon also observed in late 2017 (Figure S1). Phreatic eruptions occur through the lake and are associated with increasing SO_2/CO_2, indicating that inputs of magmatic gas play a crucial role in these eruptions (de Moor, Aiuppa, Pacheco, et al., 2016).

The present study covers the period 2013 to present, focusing on the post-2014 activity and longer-term trends, based on MultiGAS measurements, SO_2 fluxes, seismicity, and deformation. We emphasize the precursors observed prior to the 2017 eruption and propose that hydrothermal sealing played an important role in priming the system (2015–2016) for the larger explosive eruptions (2017) when magmatic activity increased.

2. Eruptive Activity

The current period of activity at Poás began in 2006 (Rymer et al., 2009). Three phases of eruptions are identified since 2012 (Figure 1). Phase 1 (2012 to 27 August 2014) produced numerous (~150) phreatic eruptions (columns ≤700 m) through the lake. Phase 2 (5 June 2016 to 17 September 2016) produced ~80 phreatic eruptions, with column heights ≤400 m. Phase 1 and 2 eruptions were similar, consisting of explosive expulsion of lake water, sediments, and altered bombs in cypresoidal columns accompanied by radial steam-rich base surges. Phase 3 (12 April 2017 to 24 September 2017) produced steam-rich eruption columns to ~4 km (Figure S1b) and culminated in the first significant expulsion of magma at Poás since 1953–1955 (Salvage et al., 2018).

Observations of the unrest preceding the 2017 eruption are insightful. On 1 April a geyser-like manifestation (locally termed "borbollón") emerged producing continuous jetting (up to ~20 m) of sediment-rich water and steam at the edge of the lake. On 7 April an additional borbollón emerged on the crater floor, producing spouts up to 5 m. The national park was closed on 9 April due to strong degassing (~400 t/day SO_2).

A small phreatic/phreatomagmatic explosion (<1 km) occurred at 8 p.m. on 12 April. The volcano produced a similar-sized eruption on 13 April at 3:45 p.m. On 14 April at 7:57 a.m. a column of ~4 km was observed, with bombs impacting the tourist overlook. A ~40-m-wide crater was formed and flooded by lake water. Small eruptions were frequent, until 22 April when a strong phreatomagmatic eruption occurred, ejecting large plastic breadcrust bombs around the vent (Figure S1c). Inspection of erupted material indicated that the early eruptive products were dominated by hydrothermally altered material, whereas later products were dominated by fresh-looking glassy clasts.

The new vent erupted semicontinuously from late April through September 2017, forming a tuff cone that occasionally inhibited the influx of crater lake water. The porous dam failed and reformed on numerous occasions. The gas and ash plume was often visibly water rich (dense white eruption column ejected through the lake). The desiccation of the crater lake in mid-June (Figure 1) revealed a canary-yellow cone of native sulfur (S; Figure S1d) and a dark gray pool of molten native S. After disappearance of the lake, ash emissions appeared drier (Figure S1e) and gradually decreased in frequency until the end of phase 3 eruptive activity in late September 2018.

3. Methods

Sulfur dioxide (SO_2) flux has been monitored at Poás since 2013 (Figure 1) following the walking traverse method of de Moor, Aiuppa, Pacheco, et al. (2016). During the 2017 eruptive crisis drones were used to determine SO_2 flux (Section S2 and Figures S2 and S3). In June 2017 two scanning DOAS instruments (Galle et al., 2010) were installed downwind of the volcano (Section S3).

Key gas ratios (SO_2/CO_2 and H_2S/SO_2) are monitored via a permanent multiple gas analyzer (MultiGAS; Aiuppa et al., 2005; Shinohara, 2005) located on the western rim of the crater (Section S1 and Figure S2). Gas ratios are calculated in real time and telemetered via radio. The prior MultiGAS station located in the crater was destroyed on 13 April 2017 by a climactic eruption. Thereafter, drones were used for measurements of gas ratios (Section S2 and Figure S3). A permanent MultiGAS was installed again once eruptive activity had diminished in November 2017. Details of the seismic and GPS networks and methods are available in Salvage et al. (2018).

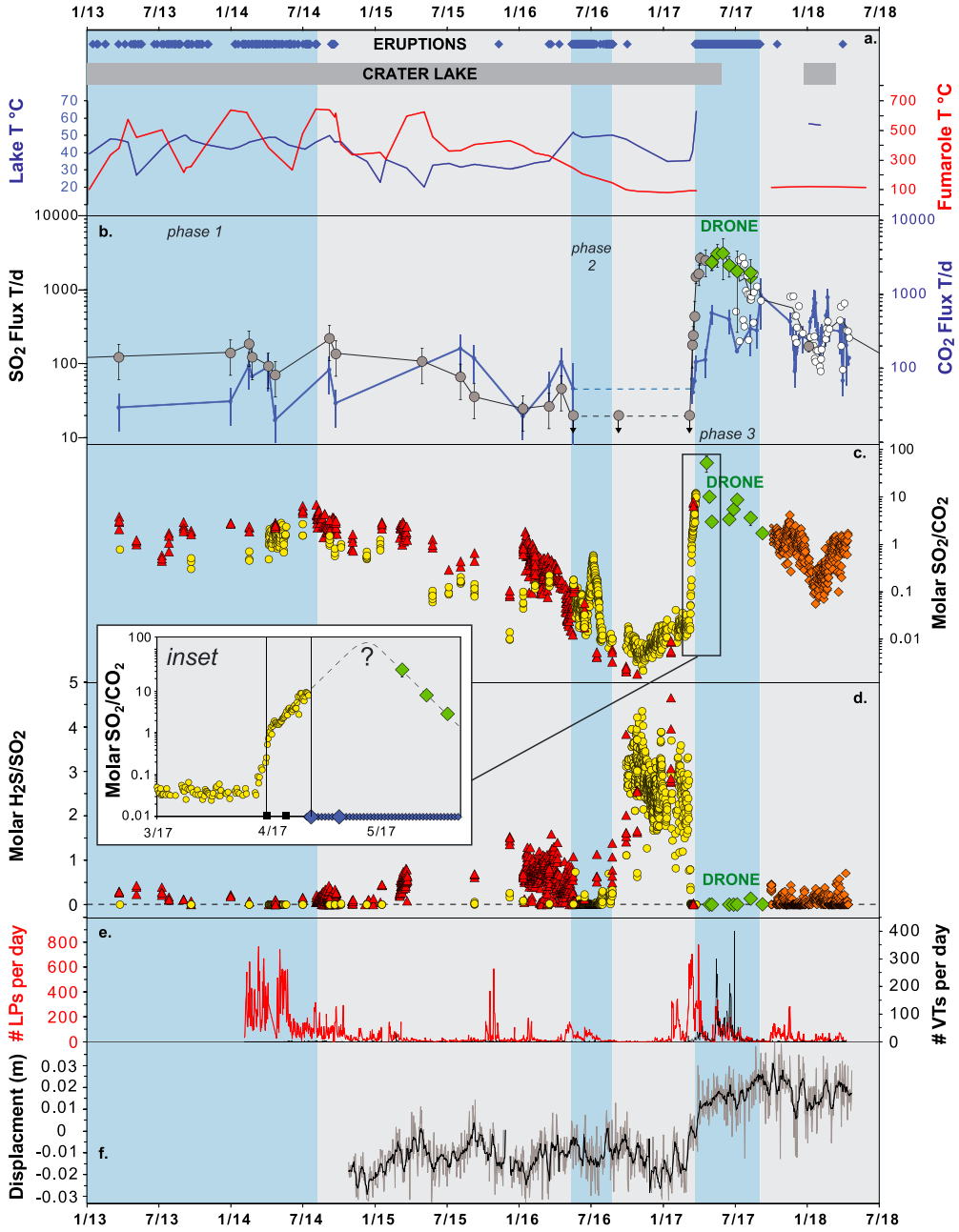

Figure 1. Time series of volcano monitoring data for Poás since 2013. Green diamonds show gas data acquired with drones in plots (b)–(d). (a) Occurrence of eruptions, presence of crater lake, and temperature data for lake and fumaroles. (b) SO_2 flux (gray circles = traverses, white circles = scanning DOAS data. Blue line shows calculated CO_2 flux (from SO_2 flux and SO_2/CO_2), with dashed section indicating period where degassing was too low (<20 t/day SO_2) for robust flux measurements. (c and d) MultiGAS data (yellow circles = lake plume, red triangles = fumarole plume, and orange diamonds = mixed plume post 2017 eruptions). (e) Seismic activity showing long period (LPs, red) and volcano tectonic (VTs, black) counts per day. (f) GPS vertical displacement data. The three eruptive phases are shown as blue shading. Inset shows zoom of MultiGAS data in run-up to 2017 eruption, where black squares are "borbollón" events and blue diamonds are eruptions. Larger blue diamonds represent eruption columns ≥4 km.

4. Results

The dynamic nature of degassing at Poás is evident through the 5-year data set (Figure 1). SO_2 fluxes have varied from below detection limit to ~3,000 t/day. SO_2/CO_2 ratios have varied over 3 orders of magnitude, from <0.03 to >30 and H_2S/SO_2 has varied from <0.01 to ~4. Though there is no obvious relationship

between lake and fumarole temperatures, their respective gas emission compositions track each other over time, consistent with changes in a common source and minimal scrubbing by the hyperacid lake (de Moor, Aiuppa, Pacheco, et al., 2016). This article considers major changes affecting the gas emissions of the bulk system.

Eruptive phase 1 was characterized by moderate SO_2 flux (70 to 220 t/day, average of 130 t/day). SO_2/CO_2 ratios were high at both the dome fumaroles and the lake gas emissions. H_2S/SO_2 was low during this period. High-frequency changes in SO_2/CO_2 in lake gas emissions were correlated with individual phreatic eruptions (de Moor, Aiuppa, Pacheco, et al., 2016). Long-period (LP) seismicity was relatively high during phase 1 with on average 227 LP events observed per day. Volcano tectonic (VT) seismicity was low with less than 1 event per day observed.

Eruptive phase 1 was followed by almost 2 years of repose with no phreatic activity. The SO_2 flux declined gradually, reaching values ~30 t/day in late 2015. SO_2/CO_2 also decreased, and H_2S became more prevalent. LP seismicity decreased to an average of 18 events per day in 2016. A GPS station was installed in late 2014 and showed oscillations in vertical displacement with an amplitude of ~2 cm with a mild overall inflation noted through the end of phase 2 eruptions.

A brief period of phreatic eruptions occurred in June to September 2016 (phase 2), accompanied by a pronounced SO_2/CO_2 peak about 1 month after the onset of eruptions, wherein values increased from 0.06 to 0.7 and then decreased to 0.03. LP seismicity demonstrated an increase in the 2 weeks prior to the onset of phase 2, with 112 events observed per day, a significant escalation over the average for the preceding repose period. Vertical displacement and VT counts did not show a significant change.

The subsequent repose period was notable due to the very low SO_2 flux (<20 t/day; Figure 1) and high H_2S/SO_2. SO_2/CO_2 ratios were exceptionally low, at values less than 0.04. LP seismicity was also low, with on average 1 event per day between the end of phase 2 and the beginning of 2017. A clear change in SO_2/CO_2 trend occurred in November 2016, from negative to positive slope, perhaps an early indicator that the probability of eruption was increasing. The change in SO_2/CO_2 slope was associated with a mild deflation event in late 2016 and early 2017. LP seismicity increased significantly in February–March 2017 (127 events per day on average), likely a result of fluid movement and overpressuring of the system (Salvage et al., 2018).

Dramatic changes in gas emissions, seismicity, and vertical displacement were observed prior to the phase 3 climactic eruptions. H_2S/SO_2 plummeted from an average of 2.4 for March to <0.01 on 31 March (Figure 1d). SO_2/CO_2 increased from ~0.04 for March to 0.10 on 30 March and 0.44 on 1 April, that is, an increase of an order of magnitude in 4 days (Figure 1 inset). These major changes were observed in both lake and fumarole gases. SO_2/CO_2 continued to increase exponentially until the eruption on 13 April, which destroyed the permanent MultiGAS station. The average SO_2/CO_2 value increased by 2 to 3 orders of magnitude in 2 weeks, at that time the largest change recorded since 2014. Though SO_2 flux data are sparse during the 5-month run-up to phase 3 due to barely detectable SO_2 emissions, the existing data show that the dramatic change in SO_2/CO_2 was paralleled by an equally dramatic increase in SO_2 flux, from <20 t/day on 28 March 2017 to 1,510 ± 290 t/day on 13 April 2017. The similarity in the magnitude and timing of the variations in SO_2/CO_2 and SO_2 flux suggest that these parameters are related (Figure 2a), although the SO_2 flux measurements suffer from relative data sparsity and detection limits that inhibit assessment of subtle changes in the run-up to phase 3 (Figure 1).

Details of the seismic behavior associated with the 2017 eruption are published in Salvage et al. (2018). To summarize, LP seismic activity peaked during the evolving crisis, reaching levels comparable to phase 1 eruptive activity in late March 2018 (Figure 1e). Notably, 704 LP events were recorded on 5 April 2017 and 776 events were recorded on 22 April 2017, the latter associated with the expulsion of magmatic bombs. VT events also increased before the onset of phase 3, with ~4 events per day in the 2 weeks prior. Many of these precursory VT events were located close to the surface, though the sparsity of seismic station precludes accurate location. The later phase 3 eruptive period was notable in terms of VT seismicity, which peaked in May–July 2017. Deformation showed inflation to 1.7 cm above background by 12 April and 3.3 cm of inflation by 20 April.

Drone flights on 10 May 2017 revealed exceptionally high average SO_2/CO_2 of 33.3 ± 11.0 ($n = 4$ with range of 21.9 to 48.7). By late May SO_2/CO_2 had dropped to 3–10. The posteruptive period was associated with $SO_2/$

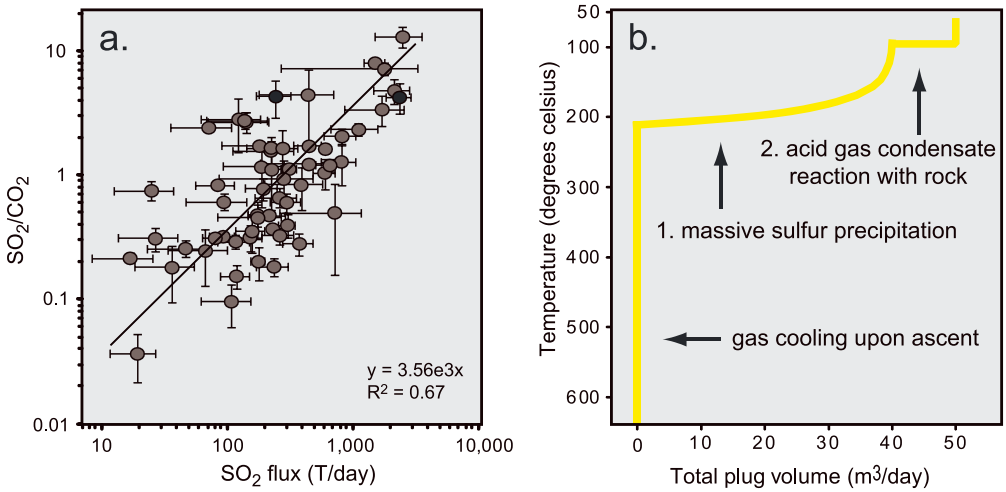

Figure 2. (a) Relationship between SO_2/CO_2 and SO_2 flux. Error bars represent 1σ standard deviation in daily averages, and two outliers (solid black symbols) were excluded from linear fit. (b) Model of hydrothermal sealing showing volume of plug formed per day, with magmatic gas input constrained by SO_2 fluxes.

CO_2 values of 0.5–3. The lake reappeared in January 2018 and was marked by a gradual decrease in SO_2/CO_2 to <0.3 and a decrease in SO_2 flux, presumably due to scrubbing in response to meteoric water influx. A change in SO_2/CO_2 trend occurred in early March 2018, associated with desiccation of the lake. A correlation is observed between daily SO_2/CO_2 measured by MultiGAS and SO_2 flux measured by DOAS (Figure 2a), suggesting that S chemistry in hydrothermal fluids and/or in magmas is driving the major observed variations.

5. Discussion

High-frequency monitoring of the 2017 phreatomagmatic eruption at Poás provides insight into eruptive triggering at hydrothermal-magmatic volcanoes. Four observations are striking (Figure 1): (1) The decrease in SO_2 flux in the 2 years prior to the eruption, (2) the large change in all monitored parameters immediately prior to the eruption, especially the precipitous drop in H_2S/SO_2 and the parallel increases in SO_2 flux and SO_2/CO_2 (Figure 2a), (3) the associated high SO_2/CO_2 ratios and VT seismicity after the initiation of the eruption (Figure 1), and (4) the subdued increase in CO_2 flux after the initiation of the eruption in combination with elevated vertical displacement in the post eruptive period. We consider two conceptual models to explain these observations. The first proposes injection of new magma as the cause of eruption. The second scenario considers hydrothermal sealing as the responsible process, through accumulation of volatiles and overpressure, ultimately leading to seal failure and eruption. Finally, we propose that these models are not mutually exclusive.

5.1. Magma Intrusion as the Eruption Driver

The 2017 eruption was the first expulsion of magma at Poás since 1953–1955. The increasing juvenile component of ash through the initial phases of the eruption (Figure S5) and the ejection of large plastic bread-crust bombs on 22 April 2017 (Figure S1) clearly demonstrate the involvement of magma in the eruption. Thus, an obvious primary consideration would be that injection of magma drove the eruption. However, juvenile bombs from the eruption are andesitic in composition—more evolved than the basaltic magma erupted in 1953–1955 (Table S2). This may suggest that a different part of the magma reservoir was mobilized during the 2017 eruption or that a basaltic intrusion into the deeper system triggered eruption of overlying andesite (e.g., Murphy et al., 2000; Pallister et al., 1992).

Gas ratios (SO_2/CO_2 and H_2S/SO_2) and SO_2 flux during the eruption suggest a very shallow magmatic source. Following the solubility degassing model of de Moor, Aiuppa, Avard, et al. (2016) for a S-rich and CO_2-poor mafic magma typical of Costa Rican volcanoes, SO_2/CO_2 values greater than 5 require equilibrium with melt at <15 MPa, indicating a shallow magma source at <500 m. SO_2/CO_2 values as high as ~15 can be

explained by magmatic degassing at ambient pressure. Carbon dioxide is less soluble than SO_2; therefore, magmatic contribution from deeper sources would drive the SO_2/CO_2 ratio down by mixing with CO_2-rich gases. Thus, the very high SO_2/CO_2 values associated with the 2017 eruption indicate that deep magma was not involved. Rather, the gas data suggest that the source was partially degassed magma previously emplaced to shallow levels (probably in late 2000, Fischer et al., 2015, to ≥500-m depth, Rymer et al., 2009), which is in also consistent with the more evolved composition of the 2017 magma. The total amount of SO_2 emitted during the eruption (~440 kT) and the average SO_2/CO_2 measured during eruptive phase 3 (4.9) can be explained by a gas phase derived from ~0.1 km^3 of partially degassed magma with ~800-ppm residual S and less than 1% of its original CO_2 (Section S4). No prior pulse of CO_2-rich magmatic gas was observed, as has been seen, for example, at Etna (Aiuppa et al., 2007), Redoubt (Werner et al., 2013), Turrialba (de Moor, Aiuppa, Avard, et al., 2016), and Masaya (Aiuppa et al., 2018). This seems to rule out intrusion of deeper basaltic magma as the eruption trigger.

Geophysical data provide further insight into the role of magma. Vertical displacement remains elevated after the eruption, indicating that a significant increase in subsurface volume occurred, likely associated with movement of magma to shallower levels (e.g., Dzurisin, 2003). The VT seismicity associated with the eruption (Salvage et al., 2018) is also consistent with magma intrusion causing changes in stress fields or propagation of pore fluid pressure leading to slip on local faults (e.g., Roman & Cashman, 2006; White & McCausland, 2016). In summary, there is no doubt that magma was involved in the 2017 eruption. Geophysical data demonstrate that magma was emplaced to shallow levels, and gas data further elucidate a shallow magmatic source for the volatiles.

5.2. Failure of the Hydrothermal Seal as an Eruption Trigger

A crucial consideration in assessing the processes driving the phase 3 activity is the preeruptive condition of the system. It is conceivable, given the lack of evidence for intrusion of CO_2-rich basaltic magma from depth, that a top-down eruption triggering mechanism also played an important role. Particularly, the gas data show evidence for hydrothermal sealing in the 2 years prior to the 2017 eruption.

The prolonged period of preeruptive decrease in SO_2 flux combined with low SO_2/CO_2 and high H_2S/SO_2 indicate hydrothermal S deposition processes (de Moor, Aiuppa, Pacheco, et al., 2016; Giggenbach, 1996; Symonds et al., 2001). Based on the decrease in SO_2 flux below background levels (roughly 150 t/day SO_2 equivalent, including H_2S emissions, and based on 2009 to 2014 data), we calculate that the S deposition rate in 2016 and early 2017 was ~14,000 m^3/year of elemental S. This value is an order of magnitude higher than the rate calculated by Rowe et al. (1992) for Poás, suggesting that hydrothermal sealing was taking place at a significantly enhanced rate in 2015–2017 (interestingly, the eruptive cycle of the 1980s studied by Rowe et al., 1992, did not culminate in magma extrusion). As described by Christenson et al. (2010), hydrothermal sealing can lead to decreased vent porosity and permeability, pressurization, and phreatic eruptions that can entrain shallow magma. In our data set, the dominance of H_2S over SO_2 in the period between phase 2 and phase 3 eruptions is powerful evidence of strong hydrothermal processes (e.g., Giggenbach, 1996) leading up to the 2017 eruption. Indeed, the rapid switch from H_2S-dominated to SO_2-dominated gases in late March 2017 was a clear sign that the system was unstable and that magmatic fluids were reaching the surface. The parallel behavior of SO_2/CO_2 and SO_2 flux (Figure 2a) further indicates that S chemistry plays a fundamentally important role in dynamic behavior at Poás and the variations in gas monitoring parameters.

Figure 2b presents a model of hydrothermal seal formation at Poás (Section S5). High T magmatic gases cool while rising through a basaltic andesite conduit. Sulfur starts precipitating at ~215 °C S, with 50% of the total SO_2 gas deposited as elemental S over a narrow temperature decrease of 25 °C (calculated using results from Rodríguez & van Bergen, 2017). As the gas cools to 100 °C, 96% of its S is deposited. Based on the decreased SO_2 flux, we calculate that this process filled ~40 m^3 of pore space per day. The steam component of the gas condenses and secondary minerals form from reaction of this acidic liquid with wall rock. The resulting hydrated mineral assemblage is silica + kaolinite + illite + hematite + anatase + pyrite + K-alunite (Rodríguez & van Bergen, 2017), which is about 10% less dense than the unaltered basaltic andesite. Thus, in situ rock alteration results in expansion that contributes to the sealing process. Considering gas cooling and condensate reaction with rock, the total sealing capacity for the pre-2017 eruption

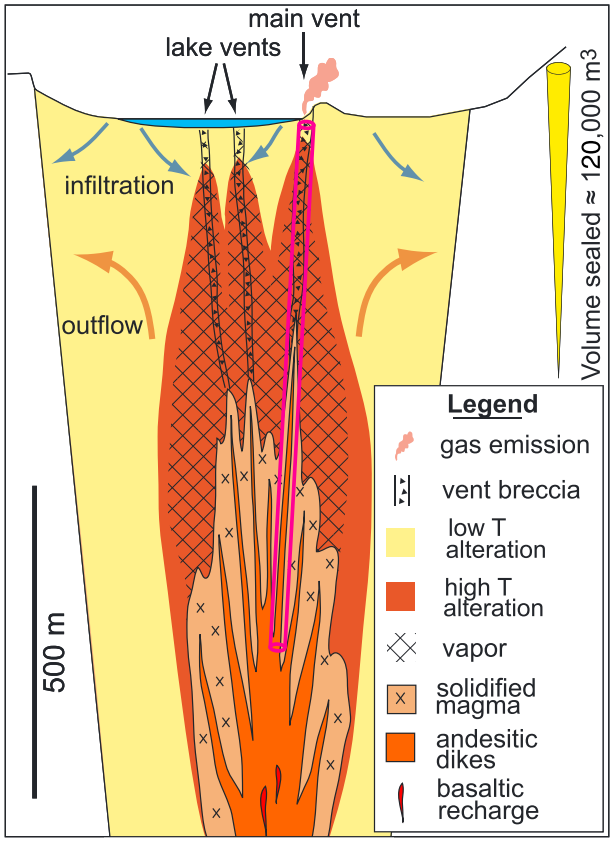

Figure 3. Schematic diagram (roughly to scale) of the Poás hydrothermal-magmatic system. Yellow cone = volume sealed prior to the 2017 eruption. Pink cylinder = approximate region of the system ejected by 2017 eruption. Prior to eruption, the upper conduits (shown as vent breccias) were sealed by hydrothermal mineralization in 2015–2017, leading to pressure accumulation in the vapor zone and more explosive behavior in phase 3 eruptions.

period is calculated at ~50 m^3/day (Figure 2b). The total volume of pore-filling secondary mineralization during the period of hydrothermal sealing (May 2015 to March 2017) is calculated at ~24,000 m^3. Considering substrate porosity of ~20% (Todesco et al., 2015), the sealed volume at Poás prior to the eruption was ~120,000 m^3 (volume of yellow cone in Figure 3). Here, it is important to note that filling of pore spaces is not expected to produce inflation as the subsurface volume does not change. Rather, the mild inflation observed between 2015 and phase 2 eruptions was more likely due to volatile accumulation below the seal, ultimately leading to its expulsion. The total modeled seal volume closely matches the estimated volume of altered material erupted in the 2017 eruption (~122,000 m^3; Section S6), lending credence to our model approach.

Thus, there is strong evidence that a hydrothermal seal formed in 2016 to early 2017 and was subsequently expelled during the opening phases of the 2017 eruption. The notable but brief increase in SO_2/CO_2 during small phase 2 eruptions (2016) is interpreted as a response of the system to sealing of the dome fumarole conduit, diverting emissions to the lake vents and driving small phreatic eruptions. This ephemeral excursion was superimposed on the longer trend of decreasing SO_2/CO_2 and increasing H_2S/SO_2 associated with sealing. The first evidence for rupture of the seal was suggested by a change in SO_2/CO_2 slope in November 2016, which was accompanied by deflation and followed by increasing LP seismicity after January 2017 (Figure 1; Salvage et al., 2018). It is notable that LP seismicity did not precede the change in SO_2/CO_2 slope. Rather, early escape of volatiles through the failing seal could have resulted in decompression boiling, generating LP events, disrupting the underlying hydrothermal-magmatic system, leading to catastrophic seal failure and massive escape of magmatic volatiles (high SO_2 fluxes). Thus, a downward propagating depressurization through the hydrothermal-magmatic system triggered by hydrothermal seal failure is hypothesized as the trigger mechanism for the 2017 eruption at Poás.

5.3. Nuanced Feedbacks Between Magmatic and Hydrothermal Processes

Magmatic gases feed hydrothermal systems, resulting in acid fluids that both dissolve rock to create porosity and precipitate secondary minerals to fill it (e.g., Varekamp et al., 2001). Magmatic heat, mostly transferred by upward migrating gases, drives vaporization of liquid water, leading to boiling pools, geyser-like exhalations, and small phreatic eruptions (Rouwet & Morrissey, 2015; Stix & de Moor, 2018). Sealing plays a crucial role in accumulation of pressure and the generation of more explosive eruptions, which can perturb and remobilize shallowly emplaced magma (Christenson et al., 2010; Giggenbach et al., 1990; Stix & de Moor, 2018).

de Moor, Aiuppa, Pacheco, et al. (2016) proposed a model for small phase 1 (2014) phreatic eruptions at Poás, whereby transient pulses of magmatic gas and heat drive vaporization leading to eruption. These small oscillations in volatile injection could be related to either magmatic processes such as variations in magma supply rate or convection rate or to opening and closing of a constriction in the magmatic or deeper hydrothermal plumbing system. Shallow hydrothermal sealing also undoubtedly plays a role in phreatic eruptions, as explosive activity requires pressure buildup in a confined space (decreased permeability) followed by energetic release when the tensile strength of the confining medium is exceeded. Small and frequent eruptions, epitomized by phase 1 activity at Poás, serve to increase permeability through fracturing, thus preventing large overpressures and promoting water influx into the conduit. In these small, geyser-like phreatic eruptions, vaporization of water by magmatic heat is thus considered the distinguishing process over hydrothermal sealing (Stix & de Moor, 2018). Enhanced hydrothermal sealing, as observed at Poás in the period leading up to the 2017 eruption, is more likely during decreased magmatic gas and heat input to the

shallow system. Under these conditions, conduits can seal more efficiently because explosive fracturing (i.e., eruptions) in the conduit is absent. If magmatic gas input then resumes, greater pressurization occurs, leading to more explosive eruptions.

We speculate that variations in the fluid flux between magmatic and hydrothermal reservoirs are intricately related with hydrothermal processes acting to seal the system, as well as to the vaporization processes driving eruptions that open conduits. Subtle variations in magma supply rate or in magma convection in the lower regions of the plumbing system likely have consequences for the upper hydrothermal system, which could prime the system for more explosive eruptions. High-frequency variations in magmatic input drive frequent small phreatic eruptions (phase 1), whereas longer-frequency variations can lead to enhanced sealing and thus larger phreatic/vulcanian eruptions when input resumes.

6. Conclusions

The efficacy of incorporating high-frequency gas monitoring into more traditional geophysical volcano monitoring programs volcanoes is demonstrated by the 5-year record at Poás. Combining geophysical methods with gas monitoring can not only provide important precursors to eruptions (rapid increase in SO_2/CO_2 and SO_2 flux, combined with inflation and increased seismicity) but also identify preeruptive processes and conditions likely to promote more explosive eruptions (hydrothermal sealing implied by low gas emissions, high H_2S/SO_2, and subtle inflation). Formation and failure of hydrothermal seals is suggested as a fundamentally important process in generating larger phreatic to phreatomagmatic eruptions and may result in top-down destabilization of hydrothermal-magmatic systems through downward propagating decompression. Phreatic explosions prior to magmatic eruptions are often considered a by-product of magma intrusion. However, in some cases hydrothermal processes may play a fundamental role in initiating magmatic eruptions. The mechanisms driving phreatic to phreatomagmatic eruptions at Poás are likely operational at many volcanoes with shallow magma and strong hydrothermal systems.

Acknowledgments

We thank Poás Volcano National Park for access and OVSICORI staff for logistical support. Julian Rüdiger, Christoph Kern, Peter Kelly, and Gaetano Giudice are thanked for their technical expertise and support. USGS-VDAP is gratefully acknowledged for providing additional scanning DOAS instruments. This work was supported by funding from the Costa Rican Ley Transitorio 8933 in support of volcano monitoring, as well as from the Deep Carbon Observatory DECADE and Biology Meets Subduction (G-2016-7206) projects. Dmitri Rouwet, Christoph Kern, an anonymous reviewer and Rebecca Carey (editor) are thanked for their helpful reviews and comments, which improved the quality of this work. Dmitri Rouwet, Christoph Kern, an anonymous reviewer, and Rebecca Carey (Editor) are thanked for their helpful reviews and comments, which improved the quality of this work. Data can be found in the supporting information and online at http://www.ovsicori.una.ac.cr/index.php/vulcanologia/estaciones-multigas).

References

Aiuppa, A., de Moor, J. M., Arellano, S., Coppola, D., Francofonte, V., Galle, B., et al. (2018). Tracking formation of a lava lake from ground and space: Masaya volcano (Nicaragua), 2014–2017. *Geochemistry, Geophysics, Geosystems*, *19*, 496–515. https://doi.org/10.1002/2017GC007227

Aiuppa, A., Federico, C., Giudice, G., & Gurrieri, S. (2005). Chemical mapping of a fumarolic field: La Fossa Crater, Vulcano Island (Aeolian Islands, Italy). *Geophysical Research Letters*, *32*, L13309. https://doi.org/10.1029/2005GL023207

Aiuppa, A., Moretti, R., Federico, C., Giudice, G., Gurrieri, S., Liuzzo, M., et al. (2007). Forecasting Etna eruptions by real-time observation of volcanic gas composition. *Geology*, *35*(12), 1115–1118. https://doi.org/10.1130/G24149A.1

Barberi, F., Bertagnini, A., Landi, P., & Principe, C. (1992). A review on phreatic eruptions and their precursors. *Journal of Volcanology and Geothermal Research*, *52*(4), 231–246. https://doi.org/10.1016/0377-0273(92)90046-G

Bogumil, K., Orphal, J., Homann, T., Voigt, S., Spietz, P., Fleischmann, O. C., et al. (2003). Measurements of molecular absorption spectra with the SCIAMACHY pre-flight model: Instrument characterization and reference data for atmospheric remote-sensing in the 230–2380 nm region. *Journal of Photochemistry and Photobiology A: Chemistry*, *157*(2-3), 167–184. https://doi.org/10.1016/S1010-6030(03)00062-5

Cashman, K. V., & Hoblitt, R. P. (2004). Magmatic precursors to the 18 May 1980 eruption of Mount St. Helens, USA. *Geology*, *32*(2), 141–144. https://doi.org/10.1130/G20078.1

Christenson, B. W., Reyes, A. G., Young, R., Moebis, A., Sherburn, S., Cole-Baker, J., & Britten, K. (2010). Cyclic processes and factors leading to phreatic eruption events: Insights from the 25 September 2007 eruption through Ruapehu Crater Lake, New Zealand. *Journal of Volcanology and Geothermal Research*, *191*(1-2), 15–32. https://doi.org/10.1016/j.jvolgeores.2010.01.008

Christenson, B. W., White, S., Britten, K., & Scott, B. J. (2017). Hydrological evolution and chemical structure of a hyper-acidic spring-lake system on Whakaari/White Island, NZ. *Journal of Volcanology and Geothermal Research*, *346*, 180–211. https://doi.org/110.1016/j.jvolgeores.2017.1006.1017

de Moor, J. M., Aiuppa, A., Avard, G., Wehrmann, H., Dunbar, N., Muller, C., et al. (2016). Turmoil at Turrialba Volcano (Costa Rica): Degassing and eruptive processes inferred from high-frequency gas monitoring. *Journal of Geophysical Research: Solid Earth*, *121*, 5761–5775. https://doi.org/10.1002/2016JB013150

de Moor, J. M., Aiuppa, A., Pacheco, J., Avard, G., Kern, C., Liuzzo, M., et al. (2016). Short-period volcanic gas precursors to phreatic eruptions: Insights from Poás Volcano, Costa Rica. *Earth and Planetary Science Letters*, *442*, 218–227. https://doi.org/10.1016/j.epsl.2016.1002.1056

de Moor, J. M., Kern, C., Avard, G., Muller, C., Aiuppa, A., Saballos, A., et al. (2017). A new sulfur and carbon degassing inventory for the Southern Central American Volcanic Arc: The importance of accurate time series datasets and implications for global volatile budgets. *Geochemistry, Geophysics, Geosystems*, *18*, 4437–4468. https://doi.org/10.1002/2017GC007141

Dzurisin, D. (2003). A comprehensive approach to monitoring volcano deformation as a window on the eruption cycle. *Reviews of Geophysics*, *41*(1), 1001. https://doi.org/10.1029/2001RG000107

Fischer, T. P., Ramirez, C., Mora-Amador, R. A., Hilton, D. R., Barnes, J. D., Sharp, Z. D., et al. (2015). Temporal variations in fumarole gas chemistry at Poás volcano, Costa Rica. *Journal of Volcanology and Geothermal Research*, *294*, 56–70. https://doi.org/10.1016/j.jvolgeores.2015.02.002

Galle, B., Johansson, M., Rivera, C., Zhang, Y., Kihlman, M., Kern, C., et al. (2010). Network for Observation of Volcanic and Atmospheric Change (NOVAC)—A global network for volcanic gas monitoring: Network layout and instrument description. *Journal of Geophysical Research*, *115*, D05304. https://doi.org/10.1029/2009JD011823

Giggenbach, W. F. (1996). Chemical composition of volcanic gas. In R. Tilling (Ed.), *IAVCEI-UNESCO: Monitoring and mitigation of volcanic hazards* (pp. 221–256). Berlin Heidelberg: Springer-Verlag. https://doi.org/10.1007/978-3-642-80087-0_7

Giggenbach, W. F., Garcia, N., Londoño, A., Rodriguez, L., Rojas, N., & Calvache, M. L. (1990). The chemistry of fumarolic vapor and thermal-spring discharges from the Nevado del Ruiz volcanic-magmatic-hydrothermal system, Colombia. *Journal of Volcanology and Geothermal Research*, *42*(1-2), 13–39. https://doi.org/10.1016/0377-0273(90)90067-P

Girona, T., Huber, C., & Caudron, C. (2018). Sensitivity to lunar cycles prior to the 2007 eruption of Ruapehu volcano. *Scientific Reports*, *8*(1), 1476. https://doi.org/10.1038/s41598-018-19307-z

Kern, C., Deutschmann, T., Vogel, L., Wöhrbach, M., Wagner, T., & Platt, U. (2009). Radiative transfer corrections for accurate spectroscopic measurements of volcanic gas emissions. *Bulletin of Volcanology*, *72*, 233–247. https://doi.org/10.1007/s00445-00009-00313-00447

Martínez, M., Fernandez, E., Valdes, J., Barboza, V., Van der Laat, R., Duarte, E., et al. (2000). Chemical evolution and volcanic activity of the active crater lake of Poás volcano, Costa Rica, 1993-1997. *Journal of Volcanology and Geothermal Research*, *97*(1-4), 127–141. https://doi.org/10.1016/S0377-0273(99)00165-1

Mastin, L. G. (1994). Explosive tephra emissions at Mount St. Helens, 1989–1991: The violent escape of magmatic gas following storms? *Geological Society of America Bulletin*, *106*(2), 175–185. https://doi.org/10.1130/0016-7606(1994)106<0175:ETEAMS>2.3.CO;2

Moretti, R., Papale, P., & Ottonello, G. (2003). A model for the saturation of C-H-O-S fluids in silicate melts. In C. Oppenheimer, et al. (Eds.), *Volcanic degassing* (pp. 81–101). London: Geol. Soc. Lond. Spec. Publ.

Murphy, M. D., Sparks, R. S. J., Barclay, J., Carroll, M. R., & Brewer, T. S. (2000). Remobilization of andesite magma by intrusion of mafic magma at the Soufriere Hills Volcano, Montserrat, West Indies. *Journal of Petrology*, *41*(1), 21–42. https://doi.org/10.1093/petrology/41.1.21

Nakamichi, H., Kumagai, H., Nakano, M., Okubo, M., Kimata, F., Ito, Y., & Obara, K. (2009). Source mechanism of a very-long-period event at Mt Ontake, central Japan: Response of a hydrothermal system to magma intrusion beneath the summit. *Journal of Volcanology and Geothermal Research*, *187*(3-4), 167–177. https://doi.org/10.1016/j.jvolgeores.2009.09.006

Oppenheimer, C., & Stevenson, D. (1989). Liquid sulfur lakes at Poás Volcano. *Nature*, *342*(6251), 790–793. https://doi.org/10.1038/342790a0

Pallister, J. S., Hoblitt, R. P., & Reyes, A. G. (1992). A basalt trigger for the 1991 eruptions of Pinatubo volcano? *Nature*, *356*(6368), 426–428. https://doi.org/10.1038/356426a0

Prosser, J. T., & Carr, M. J. (1987). Poás volcano, Costa Rica: Geology of the summit region and spatial and temporal variations among the most recent lavas. *Journal of Volcanology and Geothermal Research*, *33*(1-3), 131–146. https://doi.org/10.1016/0377-0273(87)90057-6

Rodríguez, A., & van Bergen, M. J. (2017). Superficial alteration mineralogy in active volcanic systems: An example of Poás volcano, Costa Rica. *Journal of Volcanology and Geothermal Research*, *346*, 54–80. https://doi.org/10.1016/j.jvolgeores.2017.04.006

Roman, D. C., & Cashman, K. V. (2006). The origin of volcano-tectonic earthquake swarms. *Geology*, *34*(6), 457–460. https://doi.org/10.1130/G22269.1

Rouwet, D., & Morrissey, M. M. (2015). Mechanisms of crater lake breaching eruptions. In D. Rouwet, et al. (Eds.), *Volcanic lakes* (pp. 73–91). Heidelberg: Springer.

Rouwet, D., Sandri, L., Marzocchi, W., Gottsmann, J., Selva, J., Tonini, R., & Papale, P. (2014). Recognizing and tracking volcanic hazards related to non-magmatic unrest: A review. *Journal of Applied Volcanology*, *3*(1). https://doi.org/10.1186/s13617-014-0017-3

Rowe, G. L., Brantley, S. L., Fernandez, M., Fernandez, J. F., Borgia, A., & Barquero, J. (1992). Fluid-volcano interaction in an active stratovolcano—The crater lake system of Poás Volcano, Costa-Rica. *Journal of Volcanology and Geothermal Research*, *49*(1-2), 23–51. https://doi.org/10.1016/0377-0273(92)90003-V

Rüdiger, J., Tirpitz, L., de Moor, J. M., Gutmann, A., Bobrowski, N., Liuzzo, M., & Hoffmann, T. (2018). Multicopter UAV measurements of volcanic gas emissions at Masaya (Nicaragua), Turrialba (Costa Rica), and Stromboli (Italy) volcanoes: Applications for volcano monitoring and insights into halogen speciation. *Atmospheric Measurement Techniques*, *11*(4), 2441–2457. https://doi.org/2410.5194/amt-2411-2441-2018

Rymer, H., Locke, C. A., Borgia, A., Martinez, M., Brenes, J., Van der Laat, R., & Williams-Jones, G. (2009). Long-term fluctuations in volcanic activity: Implications for future environmental impact. *Terra Nova*, *21*(4), 304–309. https://doi.org/310.1111/j.1365-3121.2009.00885.x

Salvage, R. O., Avard, G., de Moor, J. M., Pacheco, J. F., Brenes, J., Cascante, M., et al. (2018). Renewed explosive phreatomagmatic activity at Poás volcano, Costa Rica in April 2017. *Frontiers in Earth Science*, *6*, 160. https://doi.org/10.3389/feart.2018.00160

Shinohara, H. (2005). A new technique to estimate volcanic gas composition: Plume measurements with a portable multi-sensor system. *Journal of Volcanology and Geothermal Research*, *143*(4), 319–333. https://doi.org/10.1016/j.jvolgeores.2004.12.004

Stix, J., & de Moor, J. M. (2018). Understanding and forecasting phreatic eruptions driven by magma. *Earth, Planets and Space*, *70*. https://doi.org/10.1186/s40623-40018-40855-z

Stix, J., de Moor, J. M., Rüdiger, J., Alan, A., Corrales, E., D'Arcy, F., et al. (2018). Using drones and miniaturized instrumentation to study Turrialba and Masaya volcanoes, Central America. *Journal of Geophysical Research: Solid Earth*, *123*, 6501–6520. https://doi.org/10.1029/2018JB015655

Symonds, R. B., Gerlach, T. M., & Reed, M. H. (2001). Magmatic gas scrubbing: Implications for volcano monitoring. *Journal of Volcanology and Geothermal Research*, *108*(1-4), 303–341. https://doi.org/10.1016/S0377-0273(00)00292-4

Tamburello, G., Agusto, M., Caselli, A., Tassi, F., Vaselli, O., Calabrese, S., et al. (2015). Intense magmatic degassing through the lake of Copahue volcano, 2013–2014. *Journal of Geophysical Research: Solid Earth*, *120*, 6071–6084. https://doi.org/10.1002/2015JB012160

Todesco, M., Rouwet, D., Nespoli, M., & Bonafede, M. (2015). How steep is my seep? Seepage in volcanic lakes, hints from numerical simulations. In D. Rouwet, et al. (Eds.), *Volcanic lakes* (pp. 323–339). Berlin, Heidelberg: Springer.

Vandaele, A. C., Hermans, C., & Fally, S. (2009). Fourier transform measurements of SO_2 absorption cross sections: II. Temperature dependence in the 29 000–44 000 cm^{-1} (227–345 nm) region. *Journal of Quantitative Spectroscopy and Radiation Transfer*, *110*, 2115–2126. https://doi.org/10.1016/j.jqsrt.2009.2105.2006

Varekamp, J. C., Ouimette, A. P., Herman, S. W., Bermudez, A., & Delpino, D. (2001). Hydrothermal element fluxes from Copahue, Argentina: A "beehive" volcano in turmoil. *Geology*, *29*(11), 1059–1062. https://doi.org/10.1130/0091-7613(2001)029<1059:HEFFCA>2.0.CO;2

Wallace, P. J. (2005). Volatiles in subduction zone magmas: Concentrations and fluxes based on melt inclusion and volcanic gas data. *Journal of Volcanology and Geothermal Research*, *140*(1-3), 217–240. https://doi.org/10.1016/j.jvolgeores.2004.07.023

Werner, C., Kelly, P. J., Doukas, M., Lopez, T., Pfeffer, M., McGimsey, R., & Neal, C. (2013). Degassing of CO_2, SO_2, and H_2S associated with the 2009 eruption of Redoubt Volcano, Alaska. *Journal of Volcanology and Geothermal Research*, *259*, 270–284. https://doi.org/10.1016/j.jvolgeores.2012.04.012

White, R., & McCausland, W. (2016). Volcano-tectonic earthquakes: A new tool for estimating intrusive volumes and forecasting eruptions. *Journal of Volcanology and Geothermal Research*, *309*, 139–155. https://doi.org/10.1016/j.jvolgeores.2015.10.020

Zhang, Y., & Johansson, M. (2009). Mobile-DOAS software, *Gothenburg, Sweden, Chalmers University of Technology, Optical Remote Sensing Group*.